Reduced Corneal Nerve Fiber Density in Type 2 Diabetes by Wide-Area Mosaic Analysis

Neil S. Lagali,[1] Stephan Allgeier,[2] Pedro Guimarães,[3] Reza A. Badian,[4–6] Alfredo Ruggeri,[3] Bernd Köhler,[2] Tor Paaske Utheim,[4,5] Beatrice Peebo,[1] Magnus Peterson,[7] Lars B. Dahlin,[8] and Olov Rolandsson[9]

[1]Department of Ophthalmology, Institute for Clinical and Experimental Medicine, Linköping University, Linköping, Sweden
[2]Institute for Applied Computer Science, Karlsruhe Institute of Technology, Karlsruhe, Germany
[3]Department of Information Engineering, University of Padova, Padova, Italy
[4]Faculty of Health Sciences, University College of Southeast Norway, Kongsberg, Norway
[5]Department of Medical Biochemistry, Oslo University Hospital, Oslo, Norway
[6]Department of Ophthalmology, Stavanger University Hospital, Stavanger/Clinical Institute 1, Faculty of Medicine, University of Bergen, Bergen, Norway
[7]Department of Public Health and Caring Sciences, Section of Family Medicine and Preventive Medicine, Uppsala University, Uppsala, Sweden
[8]Department of Translational Medicine-Hand Surgery, Lund University, Skåne University Hospital, Malmö, Sweden
[9]Department of Public Health and Clinical Medicine, Section of Family Medicine, Umeå University, Umeå, Sweden

Correspondence: Neil S. Lagali, Department of Ophthalmology, Institute for Clinical and Experimental Medicine, Faculty of Health Sciences, Linköping University, 58183 Linköping, Sweden; neil.lagali@liu.se.

Submitted: May 20, 2017
Accepted: November 10, 2017

Citation: Lagali NS, Allgeier S, Guimarães P, et al. Reduced corneal nerve fiber density in type 2 diabetes by wide-area mosaic analysis. *Invest Ophthalmol Vis Sci*. 2017;58:6318–6327. DOI:10.1167/iovs.17-22257

Purpose. To determine if corneal subbasal nerve plexus (SBP) parameters derived from wide-area depth-corrected mosaic images are associated with type 2 diabetes.

Methods. One hundred sixty-three mosaics were produced from eyes of 82 subjects by laser-scanning in vivo confocal microscopy (IVCM). Subjects were of the same age, without (43 subjects) or with type 2 diabetes (39 subjects). Mosaic corneal nerve fiber length density (mCNFL) and apical whorl corneal nerve fiber length density (wCNFL) were quantified and related to the presence and duration of diabetes (short duration < 10 years and long duration ≥ 10 years).

Results. In mosaics with a mean size of 6 mm^2 in subjects aged 69.1 $\pm$ 1.2 years, mCNFL in type 2 diabetes was reduced relative to nondiabetic subjects (13.1 $\pm$ 4.2 vs. 15.0 $\pm$ 3.2 mm/mm^2, $P = 0.018$). Also reduced relative to nondiabetic subjects was mCNFL in both short-duration (14.0 $\pm$ 4.0 mm/mm^2, 3.2 $\pm$ 3.9 years since diagnosis) and long-duration diabetes (12.7 $\pm$ 4.2 mm/mm^2, 15.4 $\pm$ 4.2 years since diagnosis; ANOVA $P = 0.023$). Lower mCNFL was associated with presence of diabetes ($P = 0.032$) and increased hemoglobin A1c (HbA1c) levels ($P = 0.047$). By contrast, wCNFL was unaffected by diabetes or HbA1c ($P > 0.05$). Global SBP patterns revealed marked degeneration of secondary nerve fiber branches outside the whorl region in long-duration diabetes.

Conclusions. Wide-area mosaic images provide reference values for mCNFL and wCNFL and reveal a progressive degeneration of the SBP with increasing duration of type 2 diabetes.

Keywords: confocal microscopy, corneal nerves, subbasal nerve, diabetes mellitus

Recognition of the fact that the nerve fibers of the corneal subbasal nerve plexus (SBP) are axons of the peripheral nervous system has led to an increased effort in imaging, quantifying, and relating corneal nerves to the status of individuals with diabetes suffering from (or at risk of developing) diabetic peripheral neuropathy[1–5] or diabetic retinopathy.[6–9] Reduced corneal subbasal nerve fiber length density (CNFL) has been reported in subjects with type 1 and type 2 diabetes relative to healthy control subjects,[4,6,8,10–19] but reported values are based on small areas of the SBP (typically 0.16 mm^2 in size) sampled using a small number of raw in vivo confocal microscopy (IVCM) images. Prior studies also typically include subjects widely varying in age, although age is known to impact the SBP.[17,20] Moreover, an image sampling–based strategy is sensitive to selection criteria, the disease state of the SBP, and observer experience/masking. As a result, nerve fiber length density values in various cohorts differ across studies, and it has been noted in systematic reviews that better standardization of methods is required for clinical adoption of IVCM to assess pathologic levels of nerve length density.[21,22]

Although wider depictions of the SBP could reduce the variability inherent in image sampling, most clinical studies report results based on sampling of nerve data from small areas of the SBP. Notable exceptions are a study in a cohort of subjects with newly diagnosed type 2 diabetes, where mosaic images representing a mean of three or four IVCM fields of view were used,[4] and a study in healthy subjects and multiple sclerosis patients with mosaics having a mean of 7.7 fields of view.[23] In recent studies of contact lens wear, mosaics consisting of six fields of view were used.[24,25] In a single earlier study,[4] depth correction for SBP variation in the axial plane was performed whereas in other studies it is not

performed. "Depth correction" here refers to the projection of subbasal nerve paths from a volume of imaged tissue onto a single plane for further analysis. This correction could be important because single IVCM images may not optimally capture the correct plane of the subbasal plexus in a repeatable manner, and the nerves and plexus themselves may not exist in a single plane but may deviate in depth at a microscopic level. Wide-area mosaics larger in size have been used to demonstrate the potential of wide-field imaging of the SBP,[26] but the mosaicking technique used was not fully automated and was applied in only two subjects.

Recently we developed a method capable of rapid reconstruction of wide-area mosaics with depth correction of nerve fiber paths that resulted in SBP depiction with a mean size of 37 IVCM fields of view (Lagali NS, et al., manuscript submitted, 2017). In this study, the same mosaics obtained in a clinical setting are analyzed with respect to characteristics of the clinical cohort. The cohort consisted of a strict age-controlled group of healthy subjects and individuals with impaired glucose tolerance, short-, or long-duration type 2 diabetes mellitus. The relationship of new mosaic-based nerve parameters mCNFL (corneal subbasal nerve fiber length density across the entire depth-corrected mosaic area) and wCNFL (corneal subbasal nerve fiber length density in a defined circular whorl region within the depth-corrected mosaic) with the presence and duration of diabetes was investigated. Besides these quantitative parameters, mosaics also enable qualitative assessment of the SBP to examine possible effects of diabetes in altering the pattern and distribution of subbasal nerve fibers.

Methods

Study Population and Recruitment

Study participants were initially recruited in 2004 as part of the Västerbotten Intervention Programme, a large population-based study in a northern Swedish county.[27] As part of that study, a group was recruited consisting of 129 age- and sex-matched subjects aged 60 ± 1 years (age of 60 years was an inclusion criterion) with normal glucose tolerance (NGT), impaired glucose tolerance (IGT), and type 2 diabetes. Exclusion criteria included subjects with nutritional deficiencies, asymmetric neuropathy (from sciatica or stroke), or an inability to appear at the initial examination. Patients satisfying enrolment criteria were included consecutively. Full details of the initial cohort are given elsewhere.[28]

For the present study, subjects from the initial cohort were included in a 10-year follow-up examination in 2014, for which an additional ophthalmic examination was conducted at the Eye Clinic of the Skellefteå Hospital, Sweden. Ophthalmic examination and patient records were used to exclude the presence of corneal disorders, dry eye disease, or specific topical medications that could affect the corneal nerves. For subjects with unconfirmed diabetes, the status in 2014 was assessed based on two oral glucose tolerance tests taken 1 week apart, with pathologic values required on both occasions for confirmation of diabetes. The tests included fasting capillary plasma glucose (fPG) and 2-hour capillary plasma glucose (2hPG) levels. Glucose tolerance results were interpreted according to 1999 World Health Organization definitions[29] (NGT: fPG < 7.0 mM and 2hPG < 8.9 mM; IGT: fPG $<$ 7.0 mM and 2hPG ≥ 8.9 to < 12.2 mM). For subjects with confirmed type 2 diabetes from 2004, hemoglobin A1c (HbA1c) levels in 2014 taken at the Umeå University Hospital were used to confirm continued diabetes status. Blood levels of HbA1c (mmol/mol) were measured for all subjects in the cohort, along with body mass index (BMI) (kg/m^2) and smoking status (nonsmoker or history of smoking). All subjects gave written informed consent to participate, and the protocol was approved by the ethical review board of the University of Umeå, Umeå, Sweden (Ethical Application no. 2013-21-31M). The conduct of the study adhered to the tenets of the Declaration of Helsinki. A flowchart depicting inclusion of subjects from the original 2004 study and the present study is given in Figure 1.

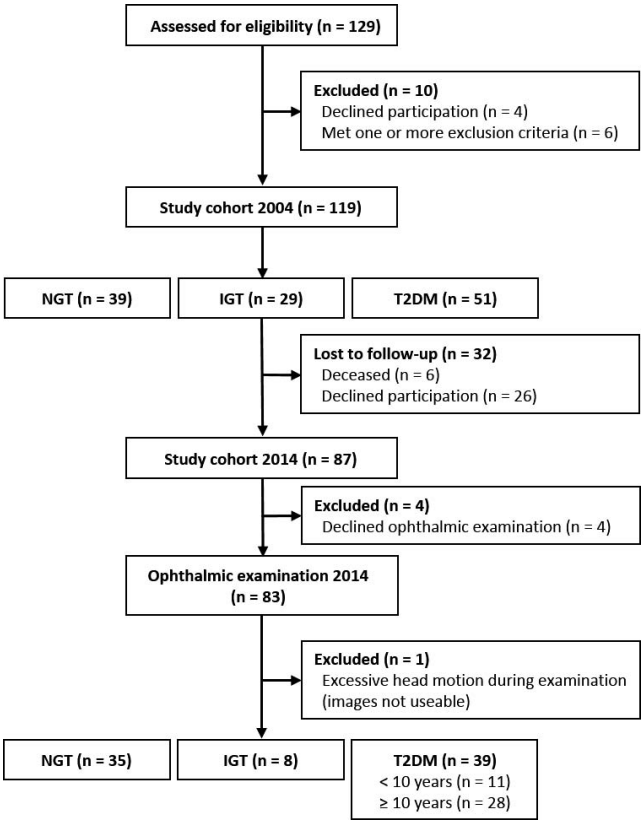

Figure 1. Study flowchart indicating original recruitment status in 2004 and study cohort for ophthalmic examination in 2014.

Confocal Microscopy and Mosaic Image Generation and Analysis

Bilateral corneal examination of study subjects was conducted during a 5-day period in January 2014 using IVCM to image the SBP (Heidelberg Retinal Tomograph 3 with Rostock Cornea Module, Heidelberg Engineering, Heidelberg, Germany). Examinations were performed by a single experienced examiner using an adaptive method of image acquisition (Lagali NS, et al., manuscript submitted, 2017). Briefly, the method involved manual raster scanning of the corneal subbasal layer with simultaneous depth scanning at each new image position (assisted by a joystick depth-control module), to create small-depth stacks of subbasal plexus images typically comprising three to five axial images at a given position. An average of 37 such positions (IVCM fields of view) per eye were scanned in this manner, representing a mean mosaic area of 6 mm^2. Raw image sets obtained by IVCM examination underwent processing by automated methods to produce depth-corrected wide-area mosaics with continuous nerve fiber paths and nerve and background intensity levels, as previously reported.[4] Also, nerves in mosaics were traced both manually and by a fully automated method[20] to quantify the total mosaic nerve fiber

Table. Clinical Characteristics of the Cohort of 82 Subjects

Characteristics	NGT	IGT	Diabetes < 10 y	Diabetes ≥ 10 y	*P* Value	Nondiabetes	Diabetes	*P* Value
No. of subjects	35	8	11	28		43	39	
Sex, % male	53	63	55	57	0.94	53	56	0.97
Smoker, %	14	38	27	36	0.22	19	33	0.20
Age, y	69.2 ± 0.7	68.5 ± 0.5	68.8 ± 0.9	69.3 ± 1.7	0.05	69.1 ± 0.7	69.1 ± 1.5	0.48
BMI, kg/m^2	25.6 ± 3.6	27.5 ± 6.7	27.8 ± 2.8	29.5 ± 4.4	**0.007***	26.0 ± 4.2	29.0 ± 4.1	**0.002**
HbA1c, mmol/mol	38.1 ± 2.8	39.6 ± 3.1	47.5 ± 6.3	57.8 ± 12.2	**< 0.00†**	38.4 ± 2.8	54.9 ± 11.8	**< 0.001**
fPG, mM	5.2 ± 0.5	6.0 ± 0.5			**0.001**	5.4 ± 0.6		
2hPG, mM	7.4 ± 1.2	11.2 ± 1.3			**< 0.001**	8.2 ± 1.9		
Mean diabetes duration, y	–	–	3.2 ± 3.9	15.4 ± 4.2	**< 0.001**	–	12.0 ± 7.4	
mCNFL, mm/mm^2	15.3 ± 3.2	14.6 ± 3.4	14.0 ± 4.0	12.7 ± 4.2	**0.030‡**	15.0 ± 3.2	13.1 ± 4.2	**0.018**
Reduction in mCNFL, mm/mm^2	–	−0.5	−1.1	−2.4		–	−1.9	
wCNFL, mm/mm^2	18.7 ± 4.6	19.0 ± 8.3	19.6 ± 3.4	18.2 ± 5.3	0.11	18.8 ± 5.1	18.7 ± 4.7	0.64

Diabetes refers to type 2 diabetes mellitus. Mean and standard deviation indicated, based on averaged bilateral data for each subject and averaged manual/automated analysis results. Reduction in mean mCNFL is relative to NGT and nondiabetes groups. *P* values represent values obtained with *t*-test (nondiabetes versus diabetes) or 1-way ANOVA (NGT, short- and long-term diabetes). wCNFL refers to whorl corneal nerve fiber length density in 800-µm diameter around whorl center. Values in bold indicate statistically significant differences between groups.

* Significant difference in BMI between NGT and diabetes ≥ 10-year group only (1-way ANOVA $P = 0.007$; Tukey post hoc test, $P = 0.003$).

† Significant differences in HbA1c between diabetes ≥ 10 years and NGT and between diabetes < 10 years and NGT (Kruskal-Wallis 1-way ANOVA on ranks $P < 0.001$; post hoc tests with Dunn's method $P < 0.05$).

‡ Significant difference in mCNFL between NGT and diabetes ≥ 10-year group only (1-way ANOVA $P = 0.030$; Tukey post hoc test, $P = 0.023$).

length density (mCNFL) and nerve fiber length density in the inferocentral whorl region (wCNFL). The total length of all traced nerves in a mosaic was divided by the mosaic area containing subbasal plexus in mm^2, yielding the mosaic corneal subbasal nerve fiber length density (mCNFL) in mm/mm^2. For the whorl region, an expert identified the center position (origin) of the whorl region in each mosaic. Then an 800-µm-diameter circular region centered on the origin was defined. Total subbasal nerve length within this region was computed and divided by the area of the circle to yield the whorl mosaic corneal subbasal nerve fiber length density (wCNFL) in mm/mm^2. Values are reported as the mean value of automated and manual tracing methods; mCNFL and wCNFL for analyses consisted of averaged values from left and right eyes of the same subject.

To understand the differences in mosaic analysis versus standard image sampling of the SBP, a comparison was performed for two scenarios. In scenario 1 (sampling with optimal depth correction), nonoverlapping 400 × 400-µm^2 square image regions were cropped from each depth-corrected mosaic; region locations were the exact locations of single images of the acquired data. The resulting mean CNFL of these cropped frames was considered. In scenario 2 (sampling of raw non–depth-corrected images), single raw images were taken from the same nonoverlapping regions identified in scenario 1. For both scenarios and 1 to 20 selected fields, mean CNFL was calculated for each possible combination of the selection (e.g., if three fields were selected, there would be 1140 possible ways to choose these three fields among a total of 20 images). Mean CNFL was then compared to the reference mCNFL to determine absolute error (in mm/mm^2) and relative error (% error referenced to mCNFL). All mosaics were computer-analyzed, and investigators at the site where nerve tracing and quantification was performed (University of Padova, Padova, Italy) were masked to the identity of subjects and subject groups.

Power Analysis

With control and diabetes groups of 40 subjects each and an expected standard deviation of ±4 mm/mm^2 in CNFL,[20] the minimum detectable difference in CNFL would be 2.5 mm/mm^2 for 80% statistical power at the 0.05 significance level. A smaller standard deviation of ±3.2 mm/mm^2 would yield a minimum detectable difference of 2 mm/mm^2.

Statistical Analysis

The cohort was stratified in two ways for the analysis, diabetes versus nondiabetes, and by duration of diabetes (NGT, IGT, short- and long-duration diabetes). Mosaic CNFL, wCNFL, and BMI in individuals with and without diabetes were compared with the independent *t*-test, while age and HbA1c were nonnormally distributed and tested with the Mann-Whitney rank sum test. Sex and smoking status were compared with the χ^2 test. Due to insufficient IGT group size to achieve statistical power of 0.80, comparisons with diabetes duration were limited to three groups (NGT, short-duration, and long-duration diabetes). Groups of NGT and short- and long-duration diabetes were assessed with 1-way ANOVA (where data was normally distributed) to compare differences in mCNFL, wCNFL, age, BMI, and HbA1c, with post hoc testing by the Tukey method. For nonnormally distributed data, the Kruskal-Wallis 1-way ANOVA on ranks was used, with Dunn's post hoc method. Sex and smoking status were assessed by the χ^2 test. Fasting plasma glucose in NGT versus IGT and diabetes duration in long- versus short-duration groups were assessed by the *t*-test after confirmation of normal distribution of the data. Linear regression was performed with mCNFL or wCNFL as the dependent variable and diabetes presence, age, BMI, sex, smoking status, and HbA1c as predictors. Power analysis was performed by the built-in Power calculation function in SigmaStat. Statistics were performed using SigmaStat 3.5 for Windows (Systat Software, Inc., Chicago, IL, USA) and IBM SPSS Statistics Ver. 23 (IBM Corp., Armonk, NY, USA) with a 2-tailed value of $\alpha < 0.05$ considered significant unless otherwise adjusted for multiple comparisons.

Results

Subject Characteristics and Examinations

A total of 164 eyes from 82 subjects were examined (Fig. 1). All eye examinations were completed during a 5-day period in an

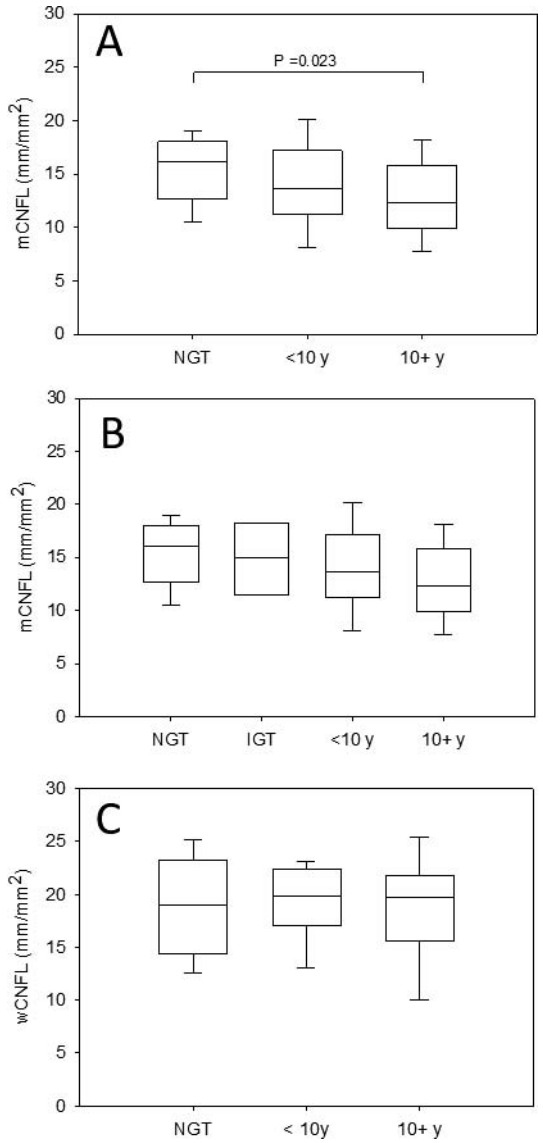

Figure 2. Relationship of mCNFL and wCNFL with onset and duration of type 2 diabetes, using the average of both eyes and both nerve tracing methods. Mosaic CNFL was based on an average of 6 mm^2 of mosaic area per eye, corresponding to 37 individual IVCM fields. (**A**) Decline in mCNFL with increasing duration of diabetes, with significant reduction in the >10-year diabetes group relative to subjects without diabetes (ANOVA $P = 0.030$, Tukey post hoc multiple comparison test $P = 0.023$). (**B**) With the IGT group included, the trend of mCNFL reduction was evident even in a prediabetes stage. (**C**) wCNFL in an 800-µm-diameter whorl region did not differ with presence or duration of diabetes. Number of subjects: 43 without diabetes (35, NGT; 8, IGT), 11 with type 2 diabetes < 10 years, 28 with type 2 diabetes ≥ 10 years. *Box plots* contain the median line and *whiskers* represent 5th and 95th percentiles.

ophthalmology outpatient clinic, representing approximately 32 eyes per day. The cohort was controlled with respect to age (69.1 ± 1.2 years, mean ± SD), and all subjects resided in the same county in northern Sweden for at least 10 years prior to examination.

Corneal Nerve Degeneration in Type 2 Diabetes

Approximately half ($n = 39$) of the study cohort of 82 subjects had a diagnosis of type 2 diabetes at the time of examination, based on the oral glucose tolerance test, while the remaining subjects ($n = 43$) did not have diabetes (having either NGT or IGT; Table). Mosaic CNFL was reduced in type 2 diabetes patients (*t*-test, $P = 0.018$) relative to those of the same age without type 2 diabetes. Mosaic CNFL was also reduced in subjects with long-duration diabetes (≥10 years) relative to equal-aged subjects with NGT (ANOVA, $P = 0.030$, Tukey post hoc test, $P = 0.023$; Fig. 2A). The trend and significance of difference between NGT and groups ≥ 10 years persisted where data from only right eyes (ANOVA $P = 0.020$; Tukey post hoc test $P = 0.015$) or only left eyes (ANOVA $P = 0.023$; Tukey post hoc test $P = 0.017$) were used. When the additional group of subjects with IGT was included, the general trend of reduced mCNFL was detected even in this group (Fig. 2B), but the group size was too small for the corresponding mCNFL difference in order to test for significance with adequate statistical power.

Whorl CNFL in an 800-µm-diameter region around the whorl center was greater than the corresponding mCNFL value in each subject group (Table); however, unlike mCNFL, wCNFL did not differ between subjects with and without diabetes (*t*-test, $P = 0.64$), nor did it change with duration of diabetes (ANOVA $P = 0.11$; Table, Fig. 2C).

In a linear regression model, mCNFL was inversely associated with having type 2 diabetes (β –0.24, $P = 0.032$, coefficient –1.803, constant 15.004). Since having a type 2 diabetes diagnosis is associated with high HbA1c, mCNFL was, as expected, also inversely associated with high HbA1c (β –0.22, $P = 0.047$, coefficient –0.072, constant 17.428). By contrast, by linear regression analysis wCNFL was not associated with the diagnosis of type 2 diabetes ($P = 0.14$) or with the level of HbA1c ($P = 0.952$).

Comparison of Standard CNFL Versus Depth-Corrected mCNFL in a Diabetes Population

The potential for error in CNFL estimation by sampling multiple single IVCM images or using raw non–depth-corrected IVCM images was investigated (Fig. 3). Sampling of multiple single IVCM images without wide-field reconstruction or depth correction led to potentially large errors in CNFL, regardless of the presence of diabetes. For scenario 1, on average, a 10% overestimation of mCNFL occurs when sampling depth-corrected IVCM images for analysis, while the potential error range is larger and increases with decreasing number of sampled images. For scenario 2, on average, a 30% underestimation of mCNFL occurs in the more common case of sampling of raw non–depth-corrected single IVCM images to determine CNFL, with the potential error range again dependent upon the actual number and location of sampled images.

Degradation of the SBP in Long-Duration Diabetes

In addition to providing quantitative measures, mosaic images revealed patterns of nerve distribution within the SBP. Comparison of mosaics from newly diagnosed subjects (diabetes diagnosed less than 1 year prior to IVCM examination) with long-term diabetes subjects (diagnosed over 20 years prior to examination) indicated a dramatic degeneration of the SBP (Fig. 4). Further qualitative comparison of mosaics from subjects with NGT and same-aged subjects with long-term diabetes indicated that within a standardized region of interest of the SBP chosen for its central proximity and as a distinguishable region with primarily vertically running nerve fibers (Fig. 5), long primary nerve fibers with prominent reflectivity were reduced in number in long-duration diabetes, while additionally many short secondary interconnecting nerve branches, normally dispersed among the main fibers, were

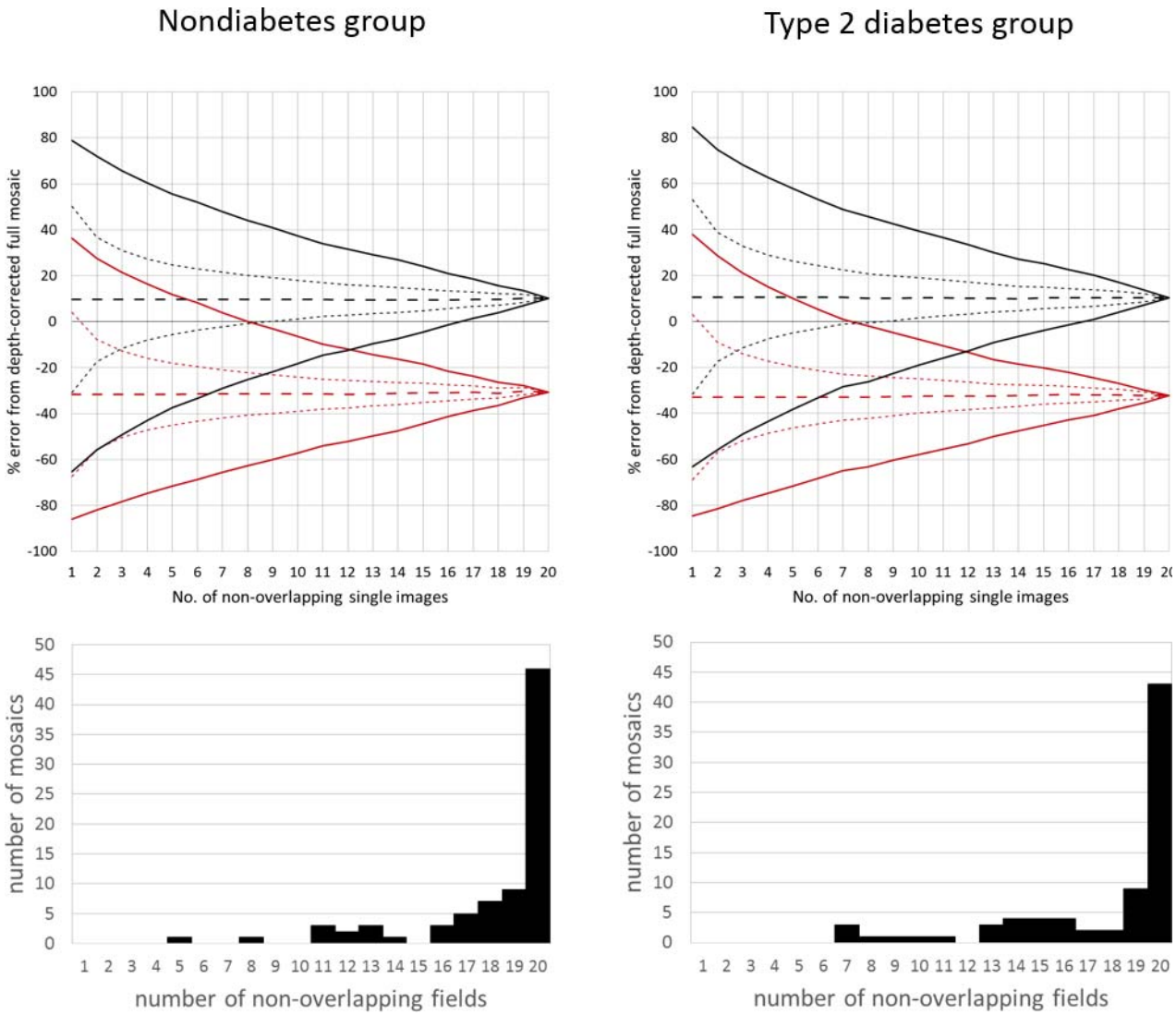

Figure 3. Subbasal corneal nerve fiber length density (CNFL) error analysis using multiple single-field sampling versus wide-field depth-corrected mosaic images (mCNFL, reference value). *Upper*: percentage error in CNFL estimation of mCNFL using various sample sizes of nonoverlapping images for healthy nondiabetes (41 subjects) and type 2 diabetes (39 subjects) groups. *Black lines* represent scenario 1, with the use of depth-corrected images (cropped from the mosaic image to the actual image positions), while *red lines* represent scenario 2, using raw, non–depth-corrected nonoverlapping IVCM images. *Dashed lines* represent the mean error in CNFL for all possible selections of the given number of sampled images relative to mCNFL, for all subjects in the group. *Dotted lines* represent the standard deviation of the error and *solid lines* represent the error limits. Positive error values are overestimates of CNFL relative to mCNFL while negative values are underestimates. *Lower*: histograms depicting the number of nonoverlapping single IVCM images within mosaics, used for the error analysis. For each group, over 50 mosaics had at least 19 nonoverlapping single image fields.

absent (Fig. 6). The short interconnecting branches in many cases lacked clear termination points at the longer nerve fibers.

Discussion

In the present cohort it was found that a lower value of the new parameter mCNFL was associated with having type 2 diabetes and that HbA1c was the mediator of this association. Whorl CNFL, however, did not show reduction with type 2 diabetes, nor was wCNFL associated with the level of HbA1c. The time elapsed after diagnosis of diabetes, however, was associated with the progressive degradation of the corneal SBP as measured by mCNFL. To our knowledge this is the first study using wide-area mosaics in a large clinical cohort, representing an area of the SBP 5^{23} to 10^4 times the area analyzed in prior cohort studies. In subjects aged 69 years in the present study, mCNFL declined by 1.9 mm/mm^2 in the diabetes group relative to those without diabetes, while the decline was 2.4 mm/mm^2 in long-duration diabetes relative to subjects with NGT. The result was robust, with a significant decline in mCNFL detected regardless of the examined eye (right, left, or both). The reduction in mCNFL of approximately 15% was, however, modest, and is notably outside the range of CNFL reduction reported in diabetes subjects relative to nondiabetes subjects in earlier studies, which all showed greater reduction in CNFL (reduction range of 3.62–6.55 mm/mm^2).[4,6,8,15,16,21] It has been pointed out in a systematic analysis, however, that these prior studies exhibited a substantial degree of heterogeneity of methods and results.[21] Additionally, in prior studies, subjects were not fixed in age, nor were wide-area mosaic images or depth correction techniques used. On the other hand, mCNFL reduction by 0.5 mm/mm^2 in an early stage of IGT relative to

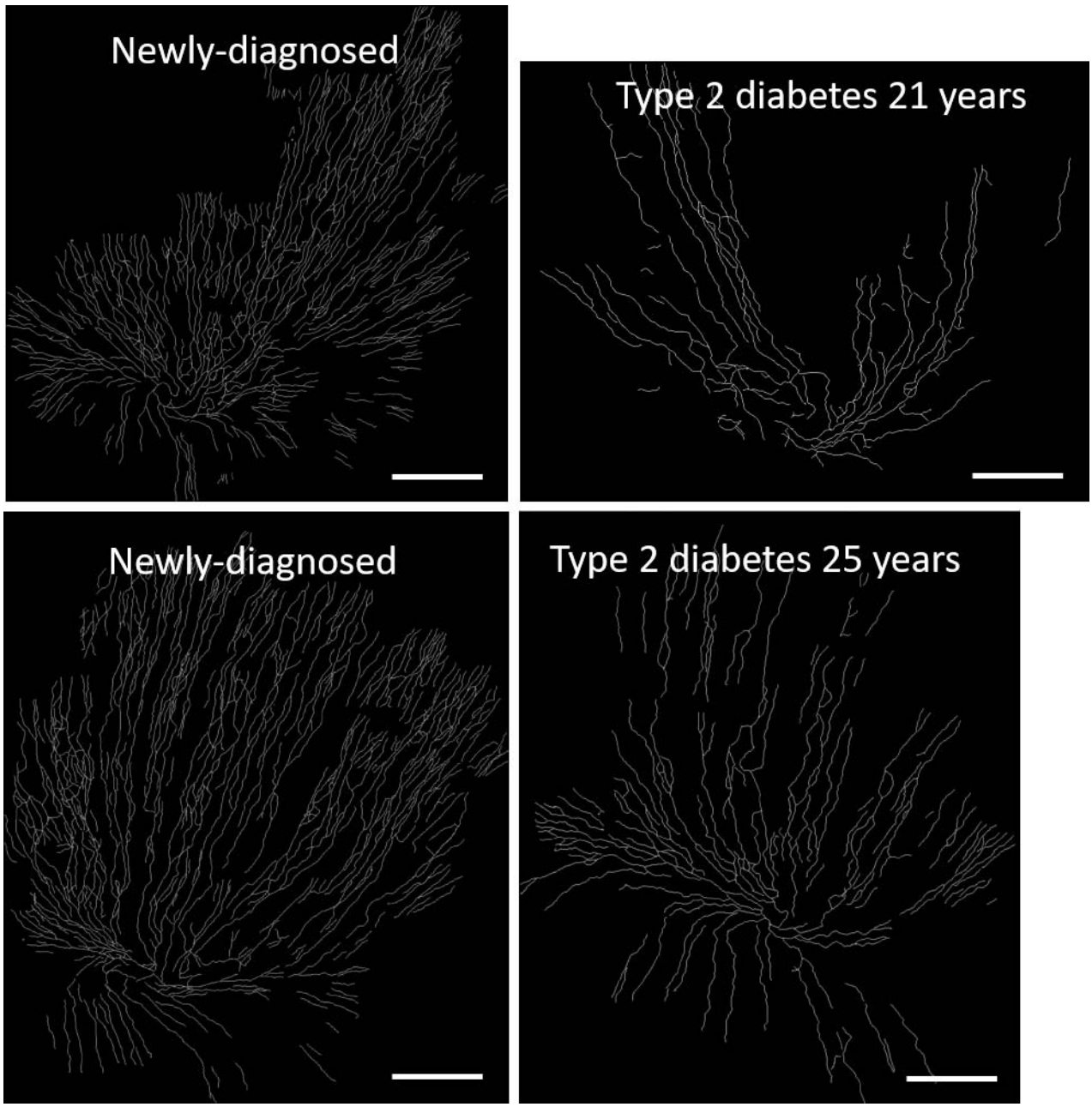

FIGURE 4. Degeneration of the subbasal nerve plexus in long-duration type 2 diabetes (two subjects, examined 21 and 25 years after first diagnosis) relative to newly diagnosed subjects (diagnosed less than 1 year prior to IVCM examination). Nerves traced from the mosaics of four study subjects are shown. A loss of nerves predominantly from outside the whorl region was evident, along with loss of short, thin nerve branch segments. *Scale bars*: 500 μm.

NGT in this study is in line with a prior report describing a modest decline of CNFL in IGT versus NGT,[30] although in the same study (not analyzing mosaics) baseline CNFL curiously increased in NGT subjects over a period of 3 years.[30]

Interestingly, the whorl density wCNFL did not vary with presence or duration of diabetes or HbA1c, but was largely preserved. In three recent studies that did not employ wide-field mosaicking or depth correction techniques,[31–33] reduced CNFL in the whorl region was reported in diabetes—a finding that could not be confirmed in our cohort. In another study, mosaic images indicated a decline in whorl density in diabetes, although the study was limited to only two subjects.[26] We attribute these discrepancies, at least in part, to differences in mosaicking, defining and analyzing the whorl area, and use of depth correction methods. As shown in the analysis of sampling with and without depth correction (Fig. 3), large errors can result from human sampling of raw IVCM images for analysis.

In the present study the visual appearance of the whorl region in mosaic images also indicated preservation of the whorl, with nerve loss appearing to occur mainly outside the whorl, through loss of highly light-scattering primary nerve fibers and, interestingly, the loss of many small, thinner interconnecting secondary nerve fiber branches. The whorl region may be more resistant to degeneration than more peripheral corneal regions as it consists of primary nerve fibers

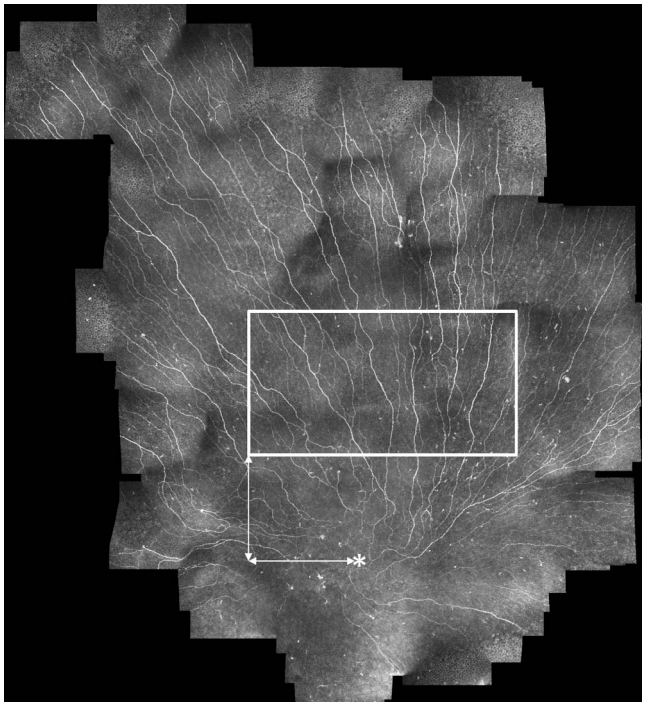

FIGURE 5. Choice of a standardized region of interest of the SBP for comparative analysis across eyes. The region of interest is chosen for its central corneal location and its ease of recognition with primarily vertically running main nerve fibers. The region size is 1100 × 650 μm (width × height) and is approximately horizontally aligned with the center of the whorl region (indicated by an *asterisk*). The exact location of the region is specified in terms of the distance from the bottom left corner to the whorl center, indicated by the *two arrows*. In this case, this region-of-interest bottom left corner is located 490 μm to the left and 488 μm above the whorl center.

arranged in a dense spiraling pattern with fewer interconnecting secondary branches, the latter possibly being more prone to degeneration. While nerve branch density (NBD) measured as the number of nerve branches per mm^2 is an IVCM parameter that has been shown to be reduced in diabetes in several studies,[4,6,8,15,34,35] the level of reduction is highly variable,[21] and NBD reflects only the number of branching points and not the actual length of the secondary branches. Secondary nerve branch length outside the apical region may therefore be an interesting parameter to concisely define and quantify in future studies, provided that a method is used to reliably image as many such branches as possible. In practice, the thin secondary nerve branches are very sensitive to the focal depth during IVCM examination and are often missed. Small adjustments in focal depth at each imaging location (as applied in the present method) produced small stacks of images that could then be projected to a single plane in order to detect the greatest possible number of secondary nerve branches. Even with this method, however, not all secondary nerve branches are visualized, due to inherent limitations of the IVCM technique.[36]

Nevertheless, a new approach was presented for systematic analysis and comparison of equivalent regions of the SBP across subjects, as shown in Figures 5 and 6. To enable future comparison across studies and longitudinally within the same subjects, a suggestion is to consistently locate and image the whorl region as a landmark, even where the whorl itself is excluded from analysis. In this manner, the exact position of images can be specified relative to the whorl center. This approach minimizes a source of variability, as it is not definitively known how certain parameters (such as CNFL and nerve fiber branching) vary regionally within the SBP. Even the use of "central corneal images" is not a well-defined concept, and in most if not all studies it cannot be verified that IVCM images chosen for analysis actually originate from the central cornea, as the IVCM hardware provides no such feedback. Using standard anatomic reference locations along with high-quality IVCM image data, automated approaches for identifying and quantifying secondary nerve branches could be employed, for example, using sophisticated algorithms as recently proposed.[37] Although the whorl position itself may not be consistent across eyes, the suggested approach for systematic analysis of the SBP referenced to the whorl location represents a step toward standardization. The whorl is an anatomic feature marking the corneal apical region. Such landmark structures in the SBP are not currently used to guide quantitative analysis of SBP parameters; images are chosen based on subjective criteria and without specific reference to SBP location.

Error analysis indicated that the potential for over- or underestimation of CNFL relative to mCNFL is significant, which may partially explain discrepancies in reported CNFL in healthy and diabetic subjects[21] relative to mCNFL values reported here. At least part of the discrepancy may be due to inclusion of the whorl region in mCNFL and its intended or unintended exclusion in other studies. Overestimation errors could also result from subjective selection of images depicting multiple, highly reflecting nerves with good contrast and ignoring those regions with sparse nerves or with only thin, secondary branches visible. Such errors may be minimized by evaluation of larger groups of subjects and reporting and comparing group means as is commonly done; however, this does not address the potentially large errors inherent in CNFL of a given single eye. Also, more effort toward a consensus regarding either inclusion or exclusion of the whorl region is needed. Thresholds for acceptable image quality and nerve visibility are also necessary, to avoid the use of images with only partial or low-quality depiction of nerves, which could impact CNFL accuracy. From the error analysis, however, an optimum number of sampled IVCM images could be proposed for a given range of acceptable error relative to mCNFL. From Figure 3, if 12 IVCM image frames are sampled, then an error range of approximately −10% to +30% would result (black lines in Fig. 3), provided that the sampled images fulfill two conditions: (1) no overlap of nerves in the 12 sampled images and (2) that each sampled image is depth-corrected, that is, a projection of a small stack of IVCM images at that location at slightly different depths. If the second condition is not met and instead 12 raw IVCM images were sampled, then the error range would be an unacceptable −50% to −10% (red lines in Fig. 3), representing an underestimation bias due to incomplete visibility of subbasal nerves in single-depth IVCM images.

A limitation of the present study was the relatively small number of individuals in the IGT and short-duration diabetes groups, which precluded a more robust statistical analysis of mCNFL changes in these stages relative to the NGT group, given the level of variance in mCNFL. This variance was just small enough to detect changes between individuals with and without diabetes or between NGT and long-term diabetes groups with sufficient power. Conversely, strengths of the present study were the high quality and large size of the wide-area mosaics, rapid imaging in a clinical setting and rapid construction and analysis of mosaics, robust analysis with automated and manual methods and left/right eyes, the number of full whorl regions imaged and quantified, and the examination of an age-controlled cohort.

In conclusion, wide-area mosaic mapping of the corneal SBP revealed a modest 15% decline in mCNFL in subjects with

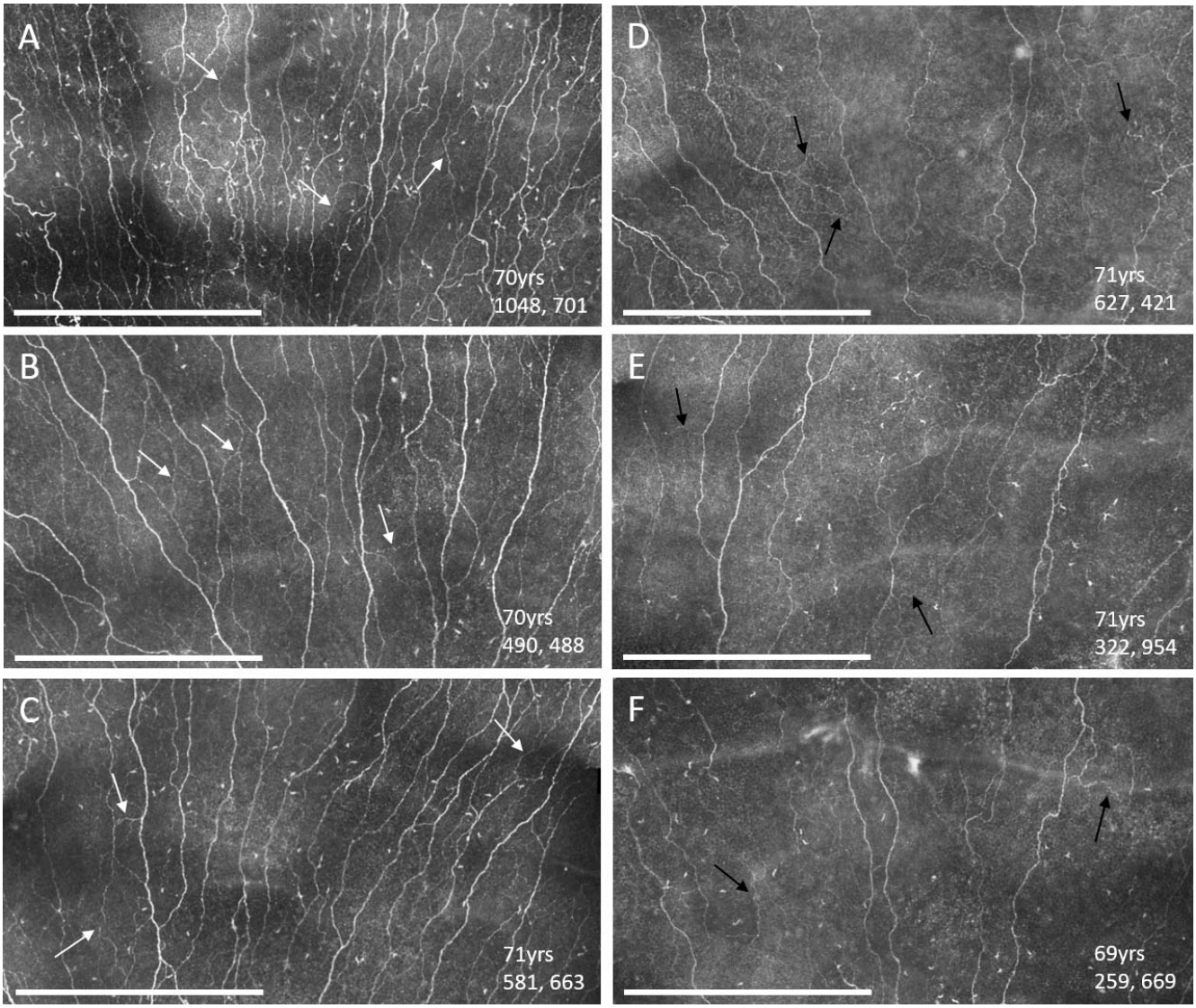

Figure 6. Loss of SBP nerve fibers in long-duration diabetes. In contrast to full mosaics used for mCNFL analysis, images here represent only a part of the full depth-corrected mosaic, cropped to equal-size image regions, to facilitate comparison between similar regions of the subbasal plexus from different subjects. Regions are compared between (**A**–**C**) nondiabetes subjects and (**D**–**F**) long-duration diabetes subjects. In subjects without diabetes, long nerve fibers were present, along with thin, short, interconnecting nerve branches (*white arrows*), which in the depth-corrected mosaics had an identifiable origin and termination point on longer main nerve fibers. By contrast, in long-duration diabetes, main nerve branches were fewer while the thin interconnecting branches were exceedingly difficult to detect even in depth-corrected mosaics, and where detected (*black arrows*), these branches did not have well-defined origins and/or termination points. All mosaic regions depicted are 1100 × 650 μm in size (width × height), with subject age and relative location of the image in microns given (distance from bottom left corner to whorl center, i.e., 1048, 701, indicates that the whorl center is 1048 μm to the right and 701 μm below the bottom left corner of the image in [**A**]). *Scale bars*: 500 μm.

diabetes over the long term. Conversely, nerve fibers of the apical whorl region (as quantified by wCNFL) were preserved in diabetes, with nerve degeneration occurring predominantly outside the whorl with an apparent loss of secondary nerve fiber branches losing their connections to the primary nerves. Analyzing depth-corrected mosaic images provides the possibility to detect and document peripheral nerve degeneration in a more robust manner than CNFL, and may represent a valuable tool in the early detection of early SBP changes in diabetes.

Acknowledgments

The authors thank Lise-Marie Ericsson at the Eye Clinic in Skellefteå, Sweden, for the kind help and support for clinical coordination and Lena Åstrom and Else-Britt Nordström for assistance with ophthalmic examinations.

The clinical examinations were supported by research funds from the Västerbotten County Council and Umeå University, Sweden (OR), Skåne University Hospital and Lund University, Sweden (LBD). The clinical imaging was supported in part by a research grant from Ögonfonden in Sweden (NSL). PG was supported by a Marie Curie grant from the European Commission in the framework of the REVAMMAD ITN (Initial Training Research network), Project number 316990. The work was also supported in part by the DFG (German Research Foundation, Grant KO 5003/1-1) and the Helmholtz Association, Germany.

Disclosure: **N.S. Lagali**, None; **S. Allgeier**, None; **P. Guimarães**, None; **R.A. Badian**, None; **A. Ruggeri**, None; **B. Köhler**, None;

T.P. Utheim, None; **B. Peebo**, None; **M. Peterson**, None; **L.B. Dahlin**, None; **O. Rolandsson**, None

References

1. Misra SL, Craig JP, Patel DV, et al. In vivo confocal microscopy of corneal nerves: an ocular biomarker for peripheral and cardiac autonomic neuropathy in type 1 diabetes mellitus. *Invest Ophthalmol Vis Sci*. 2015;56:5060–5065.
2. Pritchard N, Edwards K, Russell AW, Perkins BA, Malik RA, Efron N. Corneal confocal microscopy predicts 4-year incident peripheral neuropathy in type 1 diabetes. *Diabetes Care*. 2015;38:671–675.
3. Hossain P, Sachdev A, Malik RA. Early detection of diabetic peripheral neuropathy with corneal confocal microscopy. *Lancet*. 2005;366:1340–1343.
4. Ziegler D, Papanas N, Zhivov A, et al.; for the German Diabetes Study (GDS) Group. Early detection of nerve fiber loss by corneal confocal microscopy and skin biopsy in recently diagnosed type 2 diabetes. *Diabetes*. 2014;63:2454–2463.
5. Asghar O, Petropoulos IN, Alam U, et al. Corneal confocal microscopy detects neuropathy in subjects with impaired glucose tolerance. *Diabetes Care*. 2014;37:2643–2646.
6. Bitirgen G, Ozkagnici A, Malik RA, Kerimoglu H. Corneal nerve fibre damage precedes diabetic retinopathy in patients with type 2 diabetes mellitus. *Diabet Med*. 2014;31:431–438.
7. De Cillà S, Ranno S, Carini E, et al. Corneal subbasal nerves changes in patients with diabetic retinopathy: an in vivo confocal study. *Invest Ophthalmol Vis Sci*. 2009;50:5155–5158.
8. Nitoda E, Kallinikos P, Pallikaris A, et al. Correlation of diabetic retinopathy and corneal neuropathy using confocal microscopy. *Curr Eye Res*. 2012;37:898–906.
9. Zhivov A, Winter K, Hovakimyan M, et al. Imaging and quantification of subbasal nerve plexus in healthy volunteers and diabetic patients with or without retinopathy. *PLoS One*. 2013;8:e52157.
10. Hertz P, Bril V, Orszag A, et al. Reproducibility of in vivo corneal confocal microscopy as a novel screening test for early diabetic sensorimotor polyneuropathy. *Diabet Med*. 2011;28:1253–1260.
11. Mehra S, Tavakoli M, Kallinikos PA, et al. Corneal confocal microscopy detects early nerve regeneration after pancreas transplantation in patients with type 1 diabetes. *Diabetes Care*. 2007;30:2608–2612.
12. Tavakoli M, Mitu-Pretorian M, Petropoulos IN, et al. Corneal confocal microscopy detects early nerve regeneration in diabetic neuropathy after simultaneous pancreas and kidney transplantation. *Diabetes*. 2013;62:254–260.
13. Ahmed A, Bril V, Orszag A, et al. Detection of diabetic sensorimotor polyneuropathy by corneal confocal microscopy in type 1 diabetes: a concurrent validity study. *Diabetes Care*. 2012;35:821–828.
14. Ishibashi F, Okino M, Ishibashi M, et al. Corneal nerve fiber pathology in Japanese type 1 diabetic patients and its correlation with antecedent glycemic control and blood pressure. *J Diabetes Investig*. 2012;3:191–198.
15. Ishibashi F, Kojima R, Kawasaki A, Yamanaka E, Kosaka A, Uetake H. Correlation between sudomotor function, sweat gland duct size and corneal nerve fiber pathology in patients with type 2 diabetes mellitus. *J Diabetes Investig*. 2014;5:588–596.
16. Stem MS, Hussain M, Lentz SI, et al. Differential reduction in corneal nerve fiber length in patients with type 1 or type 2 diabetes mellitus. *J Diabetes Complications*. 2014;28:658–661.
17. Dehghani C, Pritchard N, Edwards K, et al. Morphometric stability of the corneal subbasal nerve plexus in healthy individuals: a 3-year longitudinal study using corneal confocal microscopy. *Invest Ophthalmol Vis Sci*. 2014;55:3195–3199.
18. Sivaskandarajah GA, Halpern EM, Lovblom LE, et al. Structure-function relationship between corneal nerves and conventional small-fiber tests in type 1 diabetes. *Diabetes Care*. 2013;36:2748–2755.
19. Pritchard N, Edwards K, Dehghani C, et al. Longitudinal assessment of neuropathy in type 1 diabetes using novel ophthalmic markers (LANDMark): study design and baseline characteristics. *Diabetes Res Clin Pract*. 2014;104:248–256.
20. Parissi M, Karanis G, Randjelovic S, et al. Standardized baseline human corneal subbasal nerve density for clinical investigations with laser-scanning in vivo confocal microscopy. *Invest Ophthalmol Vis Sci*. 2013;54:7091–7102.
21. De Clerck EE, Schouten JS, Berendschot TT, et al. New ophthalmologic imaging techniques for detection and monitoring of neurodegenerative changes in diabetes: a systematic review. *Lancet Diabetes Endocrinol*. 2015;3:653–663.
22. Jiang MS, Yuan Y, Gu ZX, Zhuang SL. Corneal confocal microscopy for assessment of diabetic peripheral neuropathy: a meta-analysis. *Br J Ophthalmol*. 2016;100:9–14.
23. Kheirkhah A, Muller R, Mikolajczak J, et al. Comparison of standard versus wide-field composite images of the corneal subbasal layer by in vivo confocal microscopy. *Invest Ophthalmol Vis Sci*. 2015;56:5801–5807.
24. Lum E, Golebiowski B, Swarbrick HA. Changes in corneal subbasal nerve morphology and sensitivity during orthokeratology: onset of change. *Ocul Surf*. 2017;15:227–235.
25. Golebiowski B, Chao C, Stapleton F, Jalbert I. Corneal nerve morphology, sensitivity, and tear neuropeptides in contact lens wear. *Optom Vis Sci*. 2017;94:534–542.
26. Edwards K, Pritchard N, Gosschalk K, et al. Wide-field assessment of the human corneal subbasal nerve plexus in diabetic neuropathy using a novel mapping technique. *Cornea*. 2012;31:1078–1082.
27. Norberg M, Wall S, Boman K, Weinehall L. The Västerbotten Intervention Programme: background, design and implications. *Glob Health Action*. 2010;22:3.
28. Pourhamidi K, Dahlin LB, Boman K, Rolandsson O. Heat shock protein 27 is associated with better nerve function and fewer signs of neuropathy. *Diabetologia*. 2011;54:3143–3149.
29. Alberti KG, Zimmet PZ. Definition, diagnosis and classification of diabetes mellitus and its complications. Part 1: diagnosis and classification of diabetes mellitus provisional report of a WHO consultation. *Diabet Med*. 1998;15:539–553.
30. Azmi S, Ferdousi M, Petropoulos IN, et al. Corneal confocal microscopy identifies small-fiber neuropathy in subjects with impaired glucose tolerance who develop type 2 diabetes. *Diabetes Care*. 2015;38:1502–1508.
31. Utsunomiya T, Nagaoka T, Hanada K, et al. Imaging of the corneal subbasal whorl-like nerve plexus: more accurate depiction of the extent of corneal nerve damage in patients with diabetes. *Invest Ophthalmol Vis Sci*. 2015;56:5417–5423.
32. Pritchard N, Dehghani C, Edwards K, et al. Utility of assessing nerve morphology in central cornea versus whorl area for diagnosing diabetic peripheral neuropathy. *Cornea*. 2015;34:756–761.
33. Petropoulos IN, Ferdousi M, Marshall A, et al. The inferior whorl for detecting diabetic peripheral neuropathy using corneal confocal microscopy. *Invest Ophthalmol Vis Sci*. 2015;56:2498–2504.

Investigative Ophthalmology & Visual Science

34. Chang PY, Carrel H, Huang JS, et al. Decreased density of corneal basal epithelium and subbasal corneal nerve bundle changes in patients with diabetic retinopathy. *Am J Ophthalmol*. 2006;142:488–490.
35. Mocan MC, Durukan I, Irkec M, Orhan M. Morphologic alterations of both the stromal and subbasal nerves in the corneas of patients with diabetes. *Cornea*. 2006;25:769–773.
36. Marfurt CF, Cox J, Deek S, Dvorscak L. Anatomy of the human corneal innervation. *Exp Eye Res*. 2010;90:478–492.
37. Ziegler D, Winter K, Strom A, et al. Spatial analysis improves the detection of early corneal nerve fiber loss in patients with recently diagnosed type 2 diabetes. *PLoS One*. 2017;12:e0173832.

Investigative Ophthalmology & Visual Science